Indian Journal of Pure & Applied Physics
Vol. 62, December 2024, pp. 1118-1123
DOI: 10.56042/ijpap.v62i12.12762

Electrical and Dielectric Properties of $PbO{\cdot}Bi_2O_3{\cdot}SiO_2$ Glasses

Rajni Bala[a*], Ashish Agarwal[b] & Sujata Sanghi[b]

[a]Department of Physics, Maharshi Dayanand University, Rohtak 124 001, Haryana, India
[b]Department of Physics, Guru Jambheswar University of Science and Technology, Hisar 125 001, Haryana, India

Received 25 June 2024; accepted 28 October 2024

A series of lead-bismuth silicate glasses have been made via classical melt-quench route in the compositional range $20PbO{\cdot}(80\text{-}x)Bi_2O_3{\cdot}xSiO_2$ (where, x = 10, 20, 30, and 40mol%). Impedance spectroscopy was used to collect temperature-dependent conductivity data for the glass series in the range of frequency 10Hz-7MHz and at temperatures ranging from 473K-703K. The non-Debye type nature of relaxing ions is shown by complex impedance plots. From experimental impedance data, DC conductivity; σ_{dc}, power law exponent; s, activation energy for dc conduction; E_{dc}, relaxation time; $\tau_{M''}$, activation energy for relaxation; E_τ were extracted. The dc conductivity decreased with an increase in SiO_2 content and was found to follow Arrhenius law. A close agreement in the values of activation energies determined from different formalisms suggested that during both the conduction and relaxation processes, the charge carriers must cross the similar height energy barrier.

Keywords: Bismuth silicate glasses; Conductivity, Arrhenius law; Dielectric properties; Modulus formalism

1 Introduction

Bismuth silicate glasses have gained significant attention during the past decade. The unique properties of these glasses, such as high strength, robust nonlinear optical properties, long optical region transmittance, high refractive index, corrosion resistance, and can be made in a vast range of compositions make them practically important[1-3]. Bismuth silicate glasses are very interesting for glass scientists and technologists as they cover a large area of applications such as smaller power supplies including dielectrics for supercapacitors, and electrolytes for many electrochemical devices like batteries, chemical sensors, optoelectronic devices, and smart windows[4-6]. Bismuth and lead-containing glasses find applications in optical switches, reflecting windows, optical waveguides, optical limiters, photovoltaic cells, IR-transmitting materials, high-temperature ceramic superconductors, and as radiation shielding materials[6-8]. Because of low field strength and high polarizability, Bi_2O_3 is known not to be a traditional glass former unless it is combined with another standard glass former. Depending on the type and concentration of the glass formers and modifier cations in a glass network, it may occupy the form of a former (BiO_3 units) or a modifier (BiO_6 units). Due to its dual functional ability, it can affect the electrical characteristics of oxide glasses. PbO may play a crucial role in glasses due to its capacity to create ionic and covalent connections with oxygen ions from the host matrix. It is present in many structural units within vitreous oxide systems, including the PbO_3, PbO_4, and PbO_6.

Glass-forming regions of heavy metal (Bi_2O_3, Ga_2O_3, PbO) based oxide glasses are constrained by their lesser network bond strengths when compared to conventional glasses. The addition of SiO_2 increases the chemical durability, thermal stability, and glass transition temperature of these glasses[9]. The selection of glass constituents is contingent upon their function within the glass network and their impact on the properties of glass. Studies on $PbO–ZnO–Bi_2O_3–B_2O_3–SiO_2$ glass system indicate that the change of the coordination state of Pb ion can affect the mechanical as well as structural properties of glasses[10]. Hordieiev *et al.*[11] concluded that thermal stability enhanced when SiO_2 and Bi_2O_3 were added in place of PbO. By studying the effect of adding CoO on the AC conductivity and dielectric features of lead-bismuth silicate glass system, Prasad *et al.*[12] revealed the use of glasses in display panels as transparent electrical shielding sheets. In the $TiO_2{\cdot}Bi_2O_3{\cdot}SiO_2$ system, a rise in SiO_2 content prevents polaron hopping, which lowers the conductivity of the glass system with increasing SiO_2 content[13]. Studies on

*Corresponding author:
(E-mail: khattak.rajni@gmail.com)

calcium bismuth silicate glasses indicate the existence of composition-dependent mixed former effect (MFE) on the conductivity of glasses[14].

Many investigations on the physical and optical properties of Bi_2O_3 and PbO-containing glasses have been found in the literature. However, the electrical properties of these glasses have received little consideration. This research paper aims to study the influence of Bi_2O_3 on the AC conductivity, electrical properties, and dielectric properties of 20PbO·(80-x)Bi_2O_3·xSiO_2 glasses in a wide composition and temperature range.

2. Experimental

The classical melt-quench procedure was used to synthesize the glasses with composition 20PbO·(80-x) Bi_2O_3·xSiO_2 (x = 10, 20, 30, and 40 mol %). Initially, analytical grade chemicals: PbO, Bi_2O_3, and SiO_2 were mixed thoroughly in an agate mortar. The finely grinded mixture was placed in a porcelain crucible and then in an electrical furnace maintained at 1373K for 0.5h. To achieve homogeneity, the melt was thoroughly stirred several times during melting. Finally, the resultant melt was quickly quenched between stainless steel plates. Table 1 shows the compositional ID of the samples prepared. Obtained glasses are chemically durable and moisture resistant. Electrical measurements of the samples were conducted utilizing Impedance Spectroscopy (IS). The samples were divided into square or rectangular pieces and polished with colloidal silver paint on both sides in order to evaluate the electrical conductivity. At 473K, the samples were annealed for two hours to release the internal stresses. The polished glass with silver electrode deposited was placed between the two electrodes of the sample holder, which was placed vertically in an electric furnace. AC conductivity and dielectric relaxation in all the glass samples were measured utilizing an impedance analyzer (model Newton's 4th Ltd.) in the frequency range from 10Hz-7MHz and temperature ranges from 473K-703K. The acquired data was examined using the electric modulus formalism and AC conductivity studies, as documented in the literature[15,16].

Table 1 — DC conductivity; σ_{dc}, the activation energy for dc conduction; E_{dc}, AC conductivity; σ_{ac}, and power law exponent; *s* for 20PbO·(80-x)Bi_2O_3·xSiO_2 glasses.

Glass Code	σ_{dc} (Sm^{-1}) (at 673K)	E_{dc} (eV)	σ_{ac} (Sm^{-1}) (at 673 K, 10kHZ)	s (at 673K)
PBS1	1.50×10^{-5}	1.38	2.48×10^{-5}	0.31
PBS2	1.21×10^{-5}	1.46	2.07×10^{-5}	0.34
PBS3	6.41×10^{-6}	1.51	1.11×10^{-5}	0.34
PBS4	5.41×10^{-6}	1.78	1.50×10^{-5}	0.37

$$\sigma_{ac} = 2\pi f \tan\delta \varepsilon \varepsilon_0 \quad ...(1)$$

$$\tan \delta = \frac{\varepsilon''}{\varepsilon'} \quad ...(2)$$

here, the permittivity of open space is denoted by ε_0, the dielectric loss by tanδ, and the real and imaginary components of the dielectric constant by ε' and ε'', respectively.

3. Results and discussion

3.1 DC an AC conductivity

Figure 1 displays the experimental impedance Nyquist plots for the PBS1 glass sample in the temperature range of 633K to 703K. It shows a single semicircle with the depressed center below the real (*Z'*) axis, indicating a single conduction mechanism and non-Debye nature of associated relaxation of ions[17]. Also, the radius of each semicircle is shifted towards a low value of *Z'* with the temperature rise. It indicates that the movement of charge carriers is thermally simulated in the understudy glass series. Similar plots have been observed for all other understudy samples.

Figure 2 shows the frequency-dependent total conductivity for the PBS1 glass sample at various temperatures. Frequency-dependent conductivity has been comprised of two regions; (a) the first region presents the frequency-independent part i.e. plateau

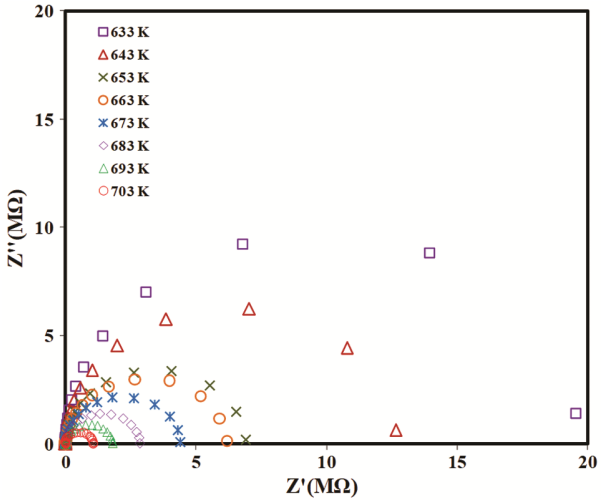

Fig. 1 — Variation of Imaginary; *Z'' vs real; Z'* parts of complex impedance for PBS1 glass (at different temperatures)

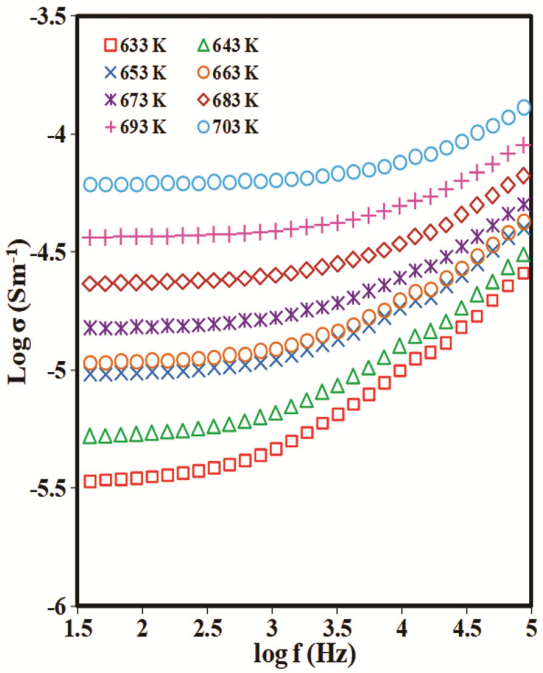

Fig. 2 — Plot of *log σ vs log f* for PBS1 glass (at different temperatures)

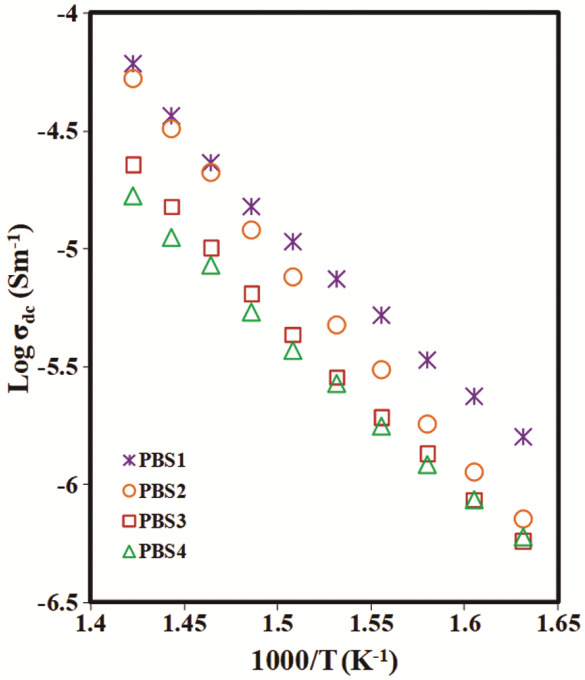

Fig. 3 — Variation of *log* σ_{dc} *vs 1000/T* for all the PBS glass samples

region (b) the second region presents the frequency-dependent part i.e. dispersive region.

At low frequencies, a plateau region appears where frequency-independent conductivity arises from the random dispersion of the charge carriers through activated hopping. Also, it is evident that as temperature rises, the transition region between the frequency-dependent and frequency-independent zones moves towards higher frequencies. Thus, the dispersion region appears at higher frequencies, where σ (ω) grows with an increase in frequency and exhibits a strong reliance on frequency. As the temperature rises, mobile ions gain more thermal energy and are able to pass through the barrier more readily, which causes the conductivity to shift towards higher frequencies[14]. Thus, a rise in temperature causes the dispersion to begin at a higher frequency.

A power law developed by Jonscher explains this dispersion in conductivity[18],

$$\sigma(\omega) = \sigma_{dc} + A\omega^{s} \quad \ldots(3)$$

where σ_{dc} = dc conductivity of the sample, s = power law exponent, and A is a frequency-independent and temperature-dependent quantity. The geometric dimensions of the samples were utilized to compute the DC conductivity (σ_{dc}), which follows Arrhenius behavior expressed as follows[19],

$$\sigma_{dc} = \sigma_0 exp\left(-\frac{E_{dc}}{k_B T}\right) \quad \ldots(4)$$

where E_{dc}= dc activation energy, k_B = Boltzmann constant, σ_0 = pre-exponential factor, and T is the absolute temperature. Variation of the log of DC conductivity with 1000/T for all the glass samples is plotted in Fig. 3, indicating the Arrhenius-type behavior. From these plots' least square fitting, the value of E_{dc} was determined from the slope of the curve.

The obtained values of σ_{dc} and E_{dc} are listed in Table 1. DC conductivity decreases while activation energy shows a reverse trend (Table 1) with an increase in SiO_2 content. In earlier studies, it was observed that Bi_2O_3 is a conditional glass former and plays the dual role of glass modifier as well as former depending upon the concentration of other constituents[4,20,21]. When SiO_2 is added at the expense of Bi_2O_3, it replaces the role of network-forming units of Bi_2O_3 with SiO_4 tetrahedral units. Thus, the dimensionality of the glass structure increases which in turn blocks the motion of cations and mobility of mobile ions and hence a decrease in conductivity is observed. Similar observations were reported by other authors in bismuth-based glasses[22-24]. Table 1 lists the values of the dimensionless frequency exponent (s),

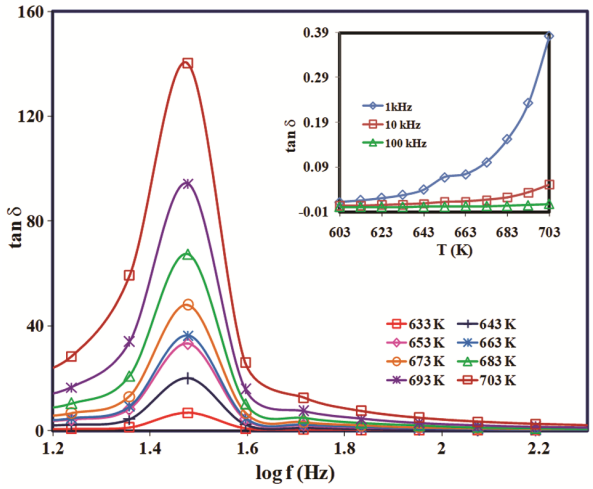

Fig. 4 — Variation of *tan δ vs log f* for PBS1 sample (at different temperatures), Inset: Plot of *tan δ vs T* for PBS1 glass sample (at different frequencies)

which are determined by calculating the slope of *log σ (ω)* vs. *log f* (Fig. 2) in the high-frequency zone. From Table 1, It can be seen that the value of *'s'* goes on increasing with an increase in the dimensionality of local conduction space and lowers the unity. Thus the value of *'s'* is material dependent.

3.2 Dielectric studies

Figure 4 illustrates the dielectric loss variation with frequency for the PBS1 glass sample at various temperatures. It may be noted that *tanδ* lies in σ_{dc} dominating (low frequency) region where loss magnitudes are higher. Magnitudes are much lower in high-frequency regions due to losses by the movement of charge carriers all through the network.

The variation of *tan δ* with temperature at various frequencies is seen in the inset of Fig. 4. These variations indicate that dielectric losses at lower frequencies are significantly higher than at higher frequencies. Because the charge carriers flow across the network under the influence of the field, which results in conduction losses. With the rise in frequency and a decrease in temperature, mobility becomes less, and a decrease in conduction losses is observed. The expected behavior of the prepared series has been similar to that observed for other bismuth-silicate glass systems[13,25].

The dielectric modulus (M^*) is given by the relation[13]

$$M^* = M' + iM'' = \frac{\varepsilon'}{(\varepsilon')^2+(\varepsilon'')^2} + i\frac{\varepsilon''}{(\varepsilon')^2+(\varepsilon'')^2} \qquad \ldots(5)$$

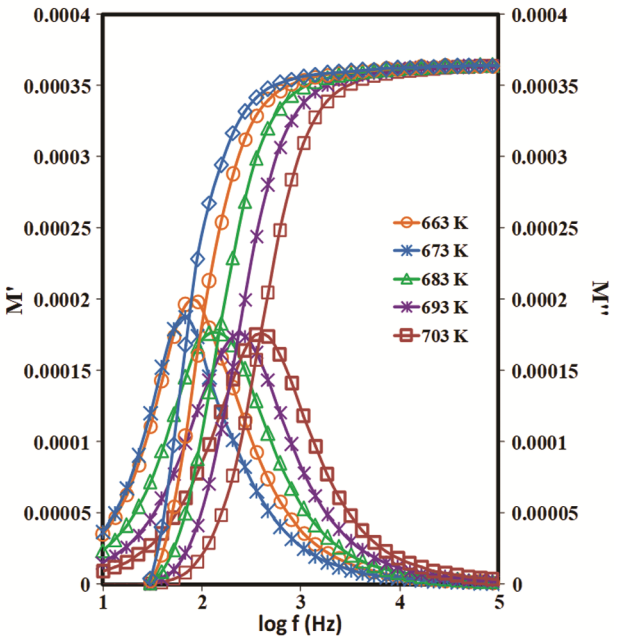

Fig. 5 — Plot of M' and M'' vs *log f* for PBS1 glass sample (at various temperatures)

where M' and M'' denote the real and imaginary parts of the electric modulus. ε' and ε'' represent the dielectric constant and dielectric loss, respectively. The electric modulus can also be expressed as the Fourier transform of a relaxation function $\phi(t)$[26]

$$M^*(\omega) = \frac{1}{\varepsilon_\infty}\left[1 - \int_0^\infty e^{-i\omega t}\left(-\frac{d\phi}{dt}dt\right)\right] \qquad \ldots(6)$$

Here, $\phi(t)$ = conductivity relaxation function, and ε_∞= represents dielectric constant at high frequency. Fig. 5 depicts the variation of M' and M'' as a function of frequency at various temperatures. At lower frequencies, M' displays very small values attributed to the ease of migration of conducting ions. M' exhibits a dispersion that tends to M_∞ at higher frequencies. Because the electric field changes quickly in this region, causing the ions to move exclusively within their potential wells and become fixed into the glass structure. The same patterns are observed for all other samples. This behavior suggests that a temperature-dependent thermally induced hopping process is thought to be responsible for charge conduction[27]. M'' reaches its maximum value in Fig. 5 at a distinctive frequency called the relaxation frequency, $f_{M''}$. It is widely recognized from the literature that long-distance mobility of charge carriers is associated with hopping conduction at frequencies lower than the relaxation frequency

($f<f_{M''}$). For frequencies greater than the relaxation frequency ($f>f_{M''}$), the charge carriers are linked to relaxation polarization processes and are movable over short distances[28]. As a result, the peak frequency, $f_{M''}$, indicates the change in mobility from long-range to short-range. Also, the values of M" shift towards a high frequency as the temperature rises, which could be the result of electrode polarization being suppressed. It shows that the relaxing process of some glass compositions is temperature-dependent.

The stretched exponential function; $\phi(t)$, representing the relaxation time distribution[29,30], is expressed as

$$\phi(t) = \phi(0)\, exp\left[-\left(\frac{t}{\tau}\right)^{\beta}\right] \quad \ldots(7)$$

where the value of β, the Kohlrausch stretched exponent, ranges from 0 to 1. The full width at half maximum value of M'' peaks has been used to evaluate the values of the β parameter. The values of β for the synthesized glass series range from 0.81 to 0.90. These values are found to be temperature-independent and not much varying for different glass samples, indicating a small departure from Debye values (β = 1). This finding implies that the glass series under study has a non-Debye type relaxing process.

In current glasses, the relation, β=1-s, is not valid due to the slight temperature dependency of exponent parameter 's'. Using the value of peak frequency, relaxation time ($\tau_{M''}$) values determined from the relation $f_{M''}$ ($=1/2\pi\tau_{M''}$) and obtained values are presented in Table 2 for all the glasses (at 673K). The slopes of the log $\tau_{M''}$ vs 1000/T plots are used to calculate the values of activation energy (E_τ) for the relaxation process. The activation energies (E_{dc} and E_τ) for each glass composition were almost equal, indicating that throughout both the conduction and relaxation processes, the charge carriers must cross the energy barrier of almost similar height.

Table 2 — The activation energy for relaxation; E_τ, dielectric loss; $tan\delta$, relaxation time; $\tau_{M''}$, and stretched exponential parameter; β for $20PbO{\cdot}(80\text{-}x)Bi_2O_3{\cdot}xSiO_2$ glasses.

Glass Code	$tan\ \delta$ (at 673K, 10 kHz)	E_τ (eV)	$\tau_{M''}$ (s) (at 673K)	β
PBS1	0.101	1.32	1.77×10^{-3}	0.81
PBS2	0.014	1.45	2.32×10^{-3}	0.84
PBS3	0.017	1.48	2.32×10^{-3}	0.81
PBS4	0.009	1.77	4.03×10^{-3}	0.90

4 Conclusion

Lead silicate glasses with varying concentrations of Bi_2O_3 have been synthesized and analyzed in terms of conduction and relaxation mechanisms. A single line of semicircle confirmed the complex nature of the cole-cole plot that shows the nature of a single conduction mechanism. As the SiO_2 content in the current glasses increases, the DC conductivity drops. This could be because more network-forming SiO_4 units increase the network dimensionality, which in turn prevents mobile ions from migrating. β parameter was found to be independent of temperature and varies between 0.81 and 0.90 for different glass samples. The activation energies calculated using various formalisms for each glass composition showed a strong consistency, indicating that during both the conduction and relaxation processes, the charge carriers must cross the energy barrier of almost similar height.

References

1 Stepien R, Pysz D, Kujawa I & Buczynski R, *Opt Mater*, 35 (2013) 1587.
2 Krishnan M L, Neethish M M & Kumar V V R K, *J Lumin*, 201 (2018) 442.
3 Geidam I G, Matori K A, Halimah M K, Chan K T, Muhammad F D, Ishak M, Umar S A & Hamza A M, *J Lumin*, 246 (2022) 118868.
4 Abdel-Hameed S A M, Mahani R, Hamzawy E M A, Almasarawi O N & Margha F H, *Silicon*, 16 (2024) 729.
5 Schmid M & Willert-Porada M, *Electrochimica Acta*, 260 (2018) e246.
6 Al-Hazmi F, Mansour S F, AlHammad M S, Abdo M A & Sadeq M S, *Ceram Int*, 47 (2021) 8566.
7 Saleh E E, Algradee M A, El-Fiki S A & Youssef G M, *Radiat Phys Chem*, 193 (2022) 109939.
8 Bala R, Agarwal A, Sanghi S & Singh N, *Opt Mater*, 36 (2013) 352.
9 Bochentyn B, Warych A, Szreder N, Mielewczyk-Gryn A, Karczewski J, Przesniak-Welenc M, Gazda M & Kusz B, *J Non-Crystalline Sol*, 439 (2016) 51.
10 Rachkovskaya G E & Zakharevich G B, *Glass Ceram*, 61 (2004) 9.
11 Hordieiev Y S & Zaichuk A V, *Res Mater*, 19 (2023) 100442.
12 Prasad V, Kostrzewa M, Gandhi Y, Ingram A, Suresh B, Reddy A S S, Kumar V R & Veeraiah N, *Phys B: Conde Matter*, 566 (2019) 136.
13 Duhan S, Sanghi S, Agarwal A, Sheoran A & Rani S, *Phys B: Cond Matter*, 404 (2009) 1648.
14 Ahlawat N, Sanghi S, Agarwal A & Ahlawat N, *Sol State Ionics*, 204 (2011) 20.
15 Yadav A, Khasa S, Hooda A, Dahiya M S, Agarwal A & Chand P, *Spectrochim Acta A*, 157 (2016) 129.
16 Szreder N A, Kupracz P, Welenc M P, Karczewski J, Gazda M, Siuzdak K & Barczyński R J, *Sol State Ionics*, 282 (2015) 37.

17 Kim J E, Kim S J & Yang Y S, *Mater Sci Eng A*, 304 (2001) 487.
18 Jonscher A K, *J Mater Sci*, 16 (1981) 2037.
19 Kalyani B, Pujari N, Edukondalu A, Reddy M S & Vardhani C P, *Mater Lett*, 317 (2022) 132128.
20 Wang P, Ye Y, Zhao G, Hou J, Liu Y, Qiao X, Wang Z, Li B & Fang Y, *J Non-Crystal Sol*, 628 (2024) 122848.
21 Gao Y, Ma J J, Chen Y & Wang M H, *J Sol-Gel Sci Technol*, 103 (2022) 713.
22 Rani S, Sanghi S, Ahlawat N & Agarwal A, *J Alloys Compd*, 619 (2015) 659.
23 Sindhu S, Sanghi S, Agarwal A, Seth V P & Kishore N , *Mater Chem Phys*, 90 (2005) 83.
24 Rani S, Sanghi S, Ahlawat N & Agarwal A, *J Mol Struct*, 1098 (2015) 1.
25 Annapurna T , Kostrzewa M , Reddy A S S, Ingram A, Ashok J, Kumar V R & Veeraiah N , *J Non-Crystal Sol*, 528 (2020) 119746.
26 Rim Y H, Lee B S, Choi H W, Cho J H & Yang Y S, J Phys Chem B, 110 (2006) 8094.
27 Morsi R M M, Ibrahim S, Naf S A & Morsi M M, *J Mater Sci Mater Electron*, 27 (2016) 4147.
28 Majhl K, Vaish R, Paramesh G & Varma K B R, *Ionics*, 19 (2012) 99.
29 Muralidharan P, Satyanarayana N & Venkateswarlu M, *Phys Chem Glass*, 46 (2005) 293.
30 El-Desokya M M & Hannora A E, *Glass Phys Chem*, 46 (2020) 487.